JOURNAL OF MATERIALS SCIENCE 22 (1987) 1031–1036

Dynamic compaction of silicon nitride powder

TAMOTSU AKASHI
Center for Explosives Technology Research, New Mexico Institute of Mining and Technology, Socorro, New Mexico 87801, USA

AKIRA B. SAWAOKA
Research Laboratory of Engineering Materials, Tokyo Institute of Technology, Yokohama 227, Japan

Dynamic compaction experiments were carried out on fine Si_3N_4 powder, that contained no additives, using maximum pressures of from 20 to 77 GPa. With pressures of from 20 to 64 GPa the relative densities of the resulting Si_3N_4 compacts were the same: 96% of the theoretical density, but their microhardness values differed significantly. The optimum shock pressure for the Si_3N_4 powder with an initial density of 60% was near 44 GPa. At this pressure, sintered Si_3N_4 compacts with a density of 96% of the theoretical density and a microhardness of 21.2 GPa were obtained. However, at 64 GPa, α-Si_3N_4 was transformed to β-Si_3N_4 as a result of the high temperatures experienced during the compaction process. Because of this transformation, the microhardness of the compacted Si_3N_4 was reduced significantly.

1. Introduction

Silicon nitride (Si_3N_4) is an attractive material for use in high-temperature structural applications because of its excellent thermal-shock, creep and oxidation resistances at high temperatures. However, major difficulties are experienced when attempts are made to consolidate Si_3N_4 powder into a dense compact by conventional sintering techniques without the use of sintering aids. These difficulties arise from the formation and growth of interparticle necks and particle coarsening before densificiation [1] caused by the strength of the materials covalent bonding. Techniques of liquid-phase sintering of Si_3N_4 powder, utilizing densification aids such as MgO, Al_2O_3 and Y_2O_3, have been developed to produce dense Si_3N_4-based ceramics [2–5]. But the high-temperature mechanical properties of the Si_3N_4 ceramics so produced are degraded by the softening of secondary phases at high temperatures [6, 7]. To retain the high creep resistance and strength of Si_3N_4 at high temperatures, a technique for the consolidation of Si_3N_4 powder into a dense compact without the use of additives is required.

Dynamic compaction is one powder compaction technique which seems to have considerable potential for the fabrication of nonoxide ceramic powders, as well as for their densification. Graham *et al.* [8] made microstructural observations of Si_3N_4 powders shock-loaded at pressures of from 11 to 17 GPa. They reported interparticle bonding and observed that the degree of this bonding increased with increasing pressure in the range 11 to 17 GPa. Recently, explosive shock compaction of α-Si_3N_4 powders was performed by Petrovic *et al.* [9]. They obtained Si_3N_4 compacts with densities of 93 to 98% of the theoretical density at pressures of 26 to 57 GPa. These results demonstrate that dynamic compaction is a promising fabrication technique for Si_3N_4 powder. However, the densification and consolidation mechanisms of Si_3N_4 powder under shock-loading conditions are not clearly understood. In this work, fine Si_3N_4 powders were dynamically compacted without sintering aids to enable a study to be made of these mechanisms.

2. Experimental procedures

2.1. Starting material

Commercial grade Si_3N_4 powder (TS-7 grade, supplied by the Toyo Soda Co. Ltd of Tokyo, Japan) was used as the starting material. The powder was a mixture of 90% α-Si_3N_4 and 10% β-Si_3N_4. The characteristics of the powder are listed in Table I. A scanning electron micrograph of the original Si_3N_4 powder (Fig. 1) shows it to be composed of loose aggregates of fine grains. The powder, which contained no densification aids, was cold-pressed at 600 MPa to form discs 5 mm thick and 12 mm in diameter. The relative densities of the discs were 60% of the theoretical density of α-Si_3N_4. The cold-pressed discs were inserted into stainless steel capsules, illustrated in Fig. 2b, and were then shock-compressed.

2.2. Dynamic compaction experiment

Shock treatments were carried out using a mouse-trap type plane-wave generator and a momentum-trap recovery system (Fig. 2a). A 4.3 mm thick iron flyer plate, illustrated in Fig. 2a, was driven onto the capsules. The impact velocities of the flyer plate employed in this experiment were 0.5, 1.1, 1.6 and 2.1 km sec^{-1}. The shock pressures induced in the Si_3N_4 samples at these impact velocities were approximated from a calculation for titanium dioxide (rutile type) powder at an impact velocity of 2.5 km sec^{-1} [10]. The approximate peak pressures obtained by scaling the pressures given by Norwood *et al.* [10] according to the impact velocities of 0.5, 1.1, 1.6 and 2.1 km sec^{-1} were 20, 44, 64, and 77 GPa.

0022–2461/87 $03.00 + .12

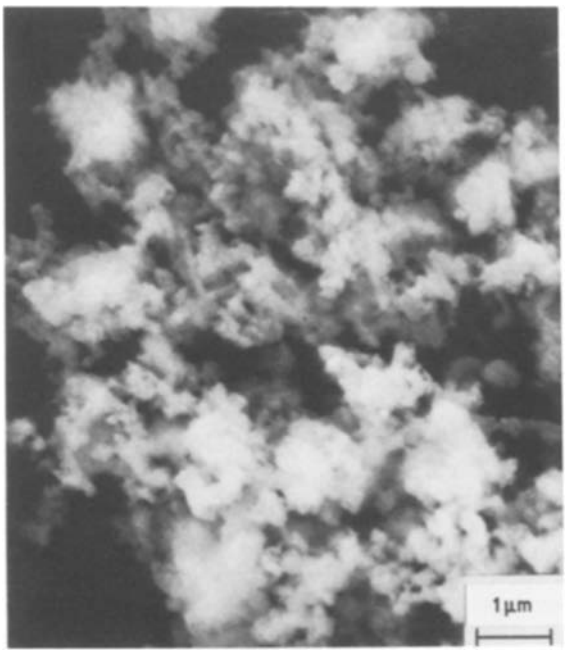

Figure 1 Scanning electron micrograph of Si_3N_4 starting powder.

Immediately after impact, the fixtures containing the capsules were plunged into water and quickly cooled before being recovered. After shock-treatment, the Si_3N_4 samples were carefully taken out of the capsules using a lathe.

2.3. Characterization of the compacted Si_3N_4

The computer calculations presented by Norwood *et al.* [10] show that in the shock-treatment fixture used the pressures and the temperatures induced by shock loading strongly depend on their positions within the powder compacts. Most noticeably, shock temperatures generated in the front and bottom regions at a given impact velocity differ significantly. These positions correspond to the direction of propagation of a shock wave. According to Norwood *et al.* [10], powder in the bottom region has a temperature about twice as high as that of powder in the front region at an impact velocity of 2.5 km sec^{-1}. In this work, therefore, the shocked Si_3N_4 powders were characterized with respect to the front and bottom regions by using X-ray diffraction, scanning electron and optical microscopy and Vicker's microhardness tester.

TABLE I Characteristics of the original Si_3N_4 powder

Average particle size (μm)	0.6 (FSSS)
Specific surface area ($m^2 g^{-1}$)	10.0 (BET)
Phase composition (wt %)	
α-Si_3N_4	90.4
β-Si_3N_4	9.6
Impurities (wt %)	
O	1.30
Cl	0.13
C	0.11
Fe	0.04
Ca	0.01
Al, Mn, Mg	< 0.01

Both surfaces of each compact were ground using a diamond wheel and then polished with 0–1 μm diamond paste. After polishing, the relative densities of the compacts were measured by means of an Archimedean method using distilled water. Vicker's microhardness was measured on the polished surfaces of the compacts using a 4.9 N load with a loading time of 15 sec. The phases present in the recovered compacts were examined using an X-ray diffractometer with a Ni-filtered Cu$K\alpha$ radiation. The residual lattice strain and the crystallite size of the compacted Si_3N_4 were determined by means of X-ray line broadening analysis using the Hall equation [11] referring to well annealed Al_2O_3 powder. X-ray diffraction patterns for the phase identification and line broadening analysis were also taken on the polished surfaces of the compacts. Microstructures of the fracture surfaces of the Si_3N_4 compacts were examined by scanning electron and optical microscopy.

3. Results and discussion

Si_3N_4 powder shock-compressed at a pressure of 77 GPa was blown out of the capsule during the dynamic-compaction process. This is probably caused by the abrupt volume expansion associated with a rarefaction wave and the decomposition of the Si_3N_4 at high temperature. Samples shock-loaded at pressures from 20 to 64 GPa were successfully recovered as discs containing several macro and microcracks (Fig. 3).

The phase compositions of Si_3N_4 in the recovered samples were determined by the method reported by

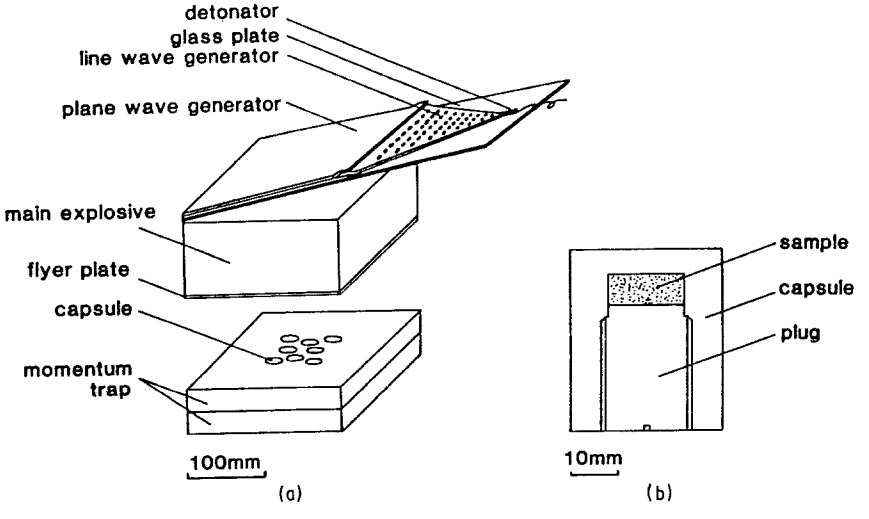

Figure 2 Arrangement for dynamic compaction: (a) plane wave generator and momentum trap recovery system; (b) stainless steel capsule.

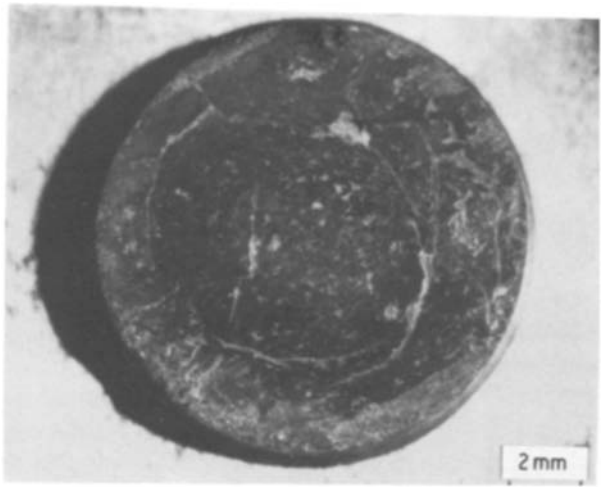

Figure 3 Sectional view of the polished front surface of Si_3N_4 compacted at 64 GPa.

Gazzara and Messier [12] using the (2 1 0) diffraction lines for α-Si_3N_4 and β-Si_3N_4. In the 20 GPa and 44 GPa shocked Si_3N_4, although a decrease in diffraction intensity and a broadening of lines for both α and β-phases were observed, there was no appreciable change in the phase composition of the Si_3N_4 resulting from shock treatment. The X-ray diffraction pattern produced by the polished front surface of the 44 GPa shocked sample is shown in Fig. 4b which can be compared to that produced by the original powder (Fig. 4a). On the other hand, in the 64 GPa shocked

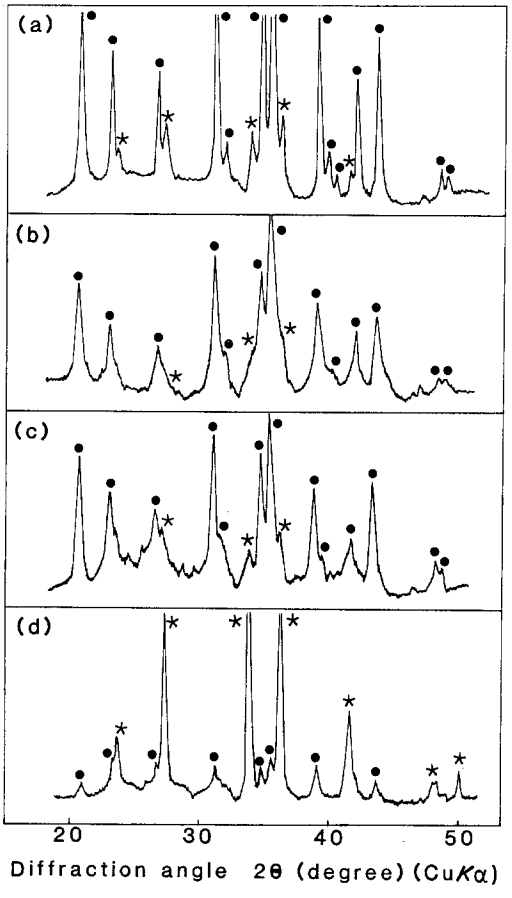

Figure 4 X-ray diffraction patterns of the original and shock-loaded Si_3N_4 powders: (a) original Si_3N_4; (b) front surface of the 44 GPa shocked Si_3N_4; (c) and (d) front (c) and bottom (d) surfaces of the 64 GPa shocked Si_3N_4. (●) α-Si_3N_4, (*) β-Si_3N_4.

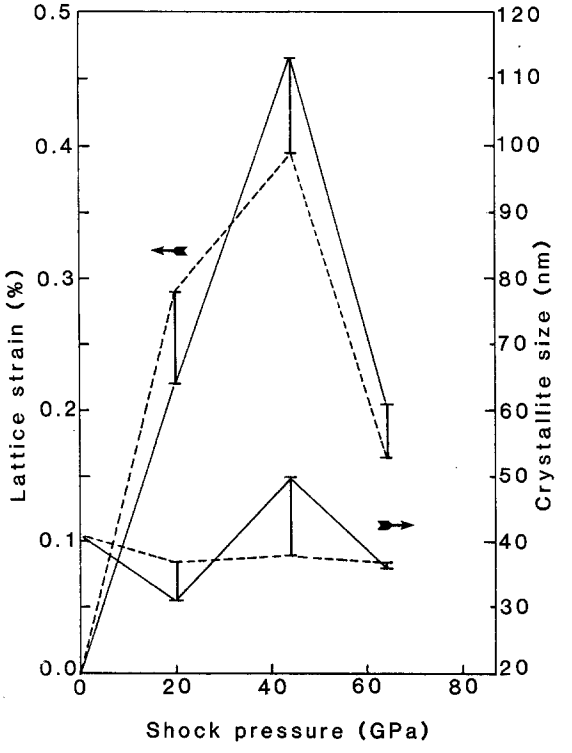

Figure 5 Crystallite size and lattice strain in shocked Si_3N_4. (——) Front, (– – –) bottom.

sample, the phase compositions of Si_3N_4 in the front and bottom surfaces were different, reflecting the difference in the pressure and temperature history of both regions during the compaction process [10]. The phase compositions of the Si_3N_4 sample were estimated to be 85% α-Si_3N_4 and 15% β-Si_3N_4 for the front surface and 22% α-Si_3N_4 and 78% β-Si_3N_4 for the bottom surface (Fig. 4c and d).

Fig. 5 shows the crystallite size and residual lattice strain of the α-phase in the Si_3N_4 powders compacted at 20, 44 and 64 GPa. These values are determined using the (1 0 1) and (2 0 2) diffraction lines of α-Si_3N_4, assuming that the coherent domains are equiaxial in the (k 0 l) directions and that the stresses are isotropic. Although the crystallite sizes obtained seem to vary slightly with pressure and position within the compacts (Fig. 5), this variation can be neglected by taking into account the experimental error incurred in determining the values in samples having large lattice strain. Thus, it is considered that in the dynamic compaction of Si_3N_4 powder having a fine crystallite size shock loading has no significant effect on the crystallite size in the pressure range of 20 to 64 GPa. However, the lattice strain values in the recovered Si_3N_4 samples exhibit the considerable effects of shock treatment of the Si_3N_4 powder. In the 20 GPa shocked sample, the lattice strain was 0.22 to 0.29% (depending on the position within the compacts). With increasing shock pressure from 20 GPa to 44 GPa, lattice strain increased additionally by a factor of about two without any appreciable change in the crystallite size. With a further increase in shock pressure from 44 GPa to 64 GPa, however, the residual strain decreased from 0.47–0.48% to 0.16–0.21%. This is apparently due to the annealing effects produced at 64 GPa as a result of the high residual

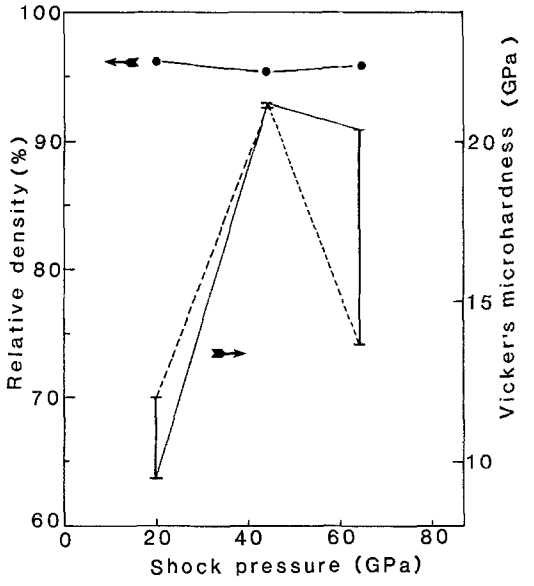

Figure 6 Relative density and Vicker's microhardness of dynamically compacted Si_3N_4. (——) Front, (– – –) bottom.

temperature. The crystallite size and lattice strain of the transformed β-Si_3N_4 were also determined by X-ray line broadening analysis using the (1 0 0) and (2 0 0) diffraction lines for β-Si_3N_4. The crystallite size was found to be 32 nm, while the residual strain was not detected within the experimental accuracy. This indicates that the α to β-phase transformation took place after shock compression.

The relative densities and microhardness values of the Si_3N_4 compacts are summarized in Fig. 6. Although these compacts were composed of α and β-phases, the relative densities in this figure were determined on the basis of the theoretical density of α-Si_3N_4 since the theoretical densities of both phases are nearly the same: $\simeq 3.18\,g\,cm^{-3}$ for α-Si_3N_4 and $\simeq 3.19\,g\,cm^{-3}$ for β-Si_3N_4 [13]. The relative densities of the compacts obtained in the pressure range of from 20 to 64 GPa were almost the same, that is, 96% of the theoretical density. This agrees well with that reported by Petrovic *et al.* [9]. They obtained Si_3N_4 compacts with densities of 93 to 98% of the theoretical density by explosive compaction of α-Si_3N_4 at pressures of from 26 to 57 GPa.

In the dynamic-compaction process, ceramic powders can be densified generally either by extensive fracture or by plastic deformation of their particles [14, 15]. The high residual strain observed in the present work and also reported by Petrovic *et al.* [9] suggests that the Si_3N_4 powder was densified by plastic deformation of the particles rather than by particle fracturing. This is the same densification mechanism as that observed in dynamic compaction of SiC and Al_2O_3 powders [15, 16]. Furthermore, considering the yield stress of Si_3N_4 at room temperature, 7 GPa, as estimated by Evans and Davidge [17], the high density obtained at 20 GPa in this work suggests that substantial densification of the Si_3N_4 powder is expected to have occurred at pressures between 7 to 20 GPa in the dynamic-compaction process. This pressure range agrees well with the range in which residual strain in compacted samples increased rapidly with pressure in the experiments of Petrovic *et al.* [9]. This agreement also suggests the densification of the Si_3N_4 powder to be by plastic deformation.

Variation in the microhardness values of the compacts with shock pressure (Fig. 6) shows that to develop strong interparticle bonding at the time of densification, higher pressures than 20 GPa, corresponding to higher temperatures, are required. As can be seen in Fig. 6, the microhardness of the Si_3N_4 compacts increases significantly with increasing shock pressure from 20 GPa to 44 GPa. The maximum microhardness value, 21.2 GPa, was obtained in the 44 GPa shocked sample. This value is equivalent to those reported for hot pressed or high-pressure hot pressed Si_3N_4 compacts without densification aids [18]. This microhardness value also corresponds to about 70% of the microhardness of chemical vapour deposited (CVD) α-Si_3N_4 [13], which is considered to be a highly pure, dense α-Si_3N_4 sintered compact. This indicates that some self-bonding developed in the shock-compacted Si_3N_4 at the time of densification at a pressure of 44 GPa. On the other hand, the microhardness values of the 64 GPa shocked sample decreased slightly in the front surface and rapidly in the bottom surface when compared to those of the 44 GPa shocked sample. This seems to be partially caused by the α-to-β transformation in this compact, because it has been reported that a single crystal of α-Si_3N_4 is about 28% harder than that of β-Si_3N_4 [13]. This reduction in microhardness may also be due to a microstructural change accompanied by the phase transformation (Fig. 9a and b).

Figs 7, 8 and 9 show typical scanning electron micrographs of the fracture surfaces in the centre parts of the front (a) and bottom (b) regions for the Si_3N_4 compacts obtained at 20, 44 and 64 GPa. In the front region of the 20 GPa compacted sample, Si_3N_4 powder with a particle size of 0.6 μm in the starting material (Fig. 1) was just compacted into loose-bonded agglomerates. Bonding between grains appears to be weak. On the other hand, the bottom region of this compact (at 20 GPa), where the powder experienced a higher temperature than in the front region, consisted of relatively dense aggregates of almost the same size as those observed in the front region. These aggregates were apparently joined to each other, but the fracture surface of this region was still mostly intergranular (Fig. 7b).

Judging from a flat and smooth morphology in the fracture surface, transgranular fracture in densely compacted regions occurred in the 44 GPa shocked sample. This fracture morphology apparently increased from the front region to the bottom region in this compact (Fig. 8a and b). This tendency corresponds to an increase in the shock and residual temperatures within the powder compact, indicating that the degree and strength of the interparticle bonding increased with increasing temperature during the shock-compaction process. This is consistent with the results of Graham *et al.* [8]. They reported that the amount of bonding in compacted Si_3N_4 increased with increasing shock pressure from 11 to 17 GPa. However, in the 64 GPa shocked sample, microhardness decreased and

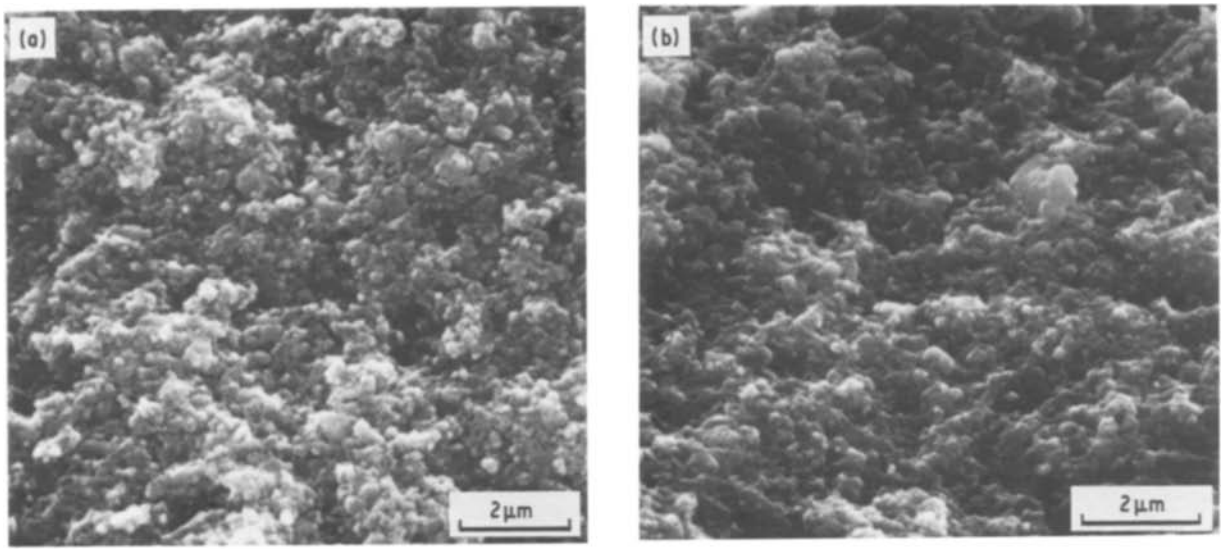

Figure 7 Scanning electron micrographs of a fracture surface of the 20 GPa shocked Si_3N_4: (a) front region; (b) bottom region.

the microstructure was changed, when compared to those of the compact obtained at 44 GPa. The front region of this compact (at 64 GPa) consisted of dense regions about 1 μm size (see the arrows in Fig. 9a), and fine grains with a relatively uniform size of from 0.2 to 0.3 μm. This microstructure shows that recrystallization of heavily deformed Si_3N_4 grains began to occur in densely compacted regions due to a high residual temperature. On the other hand, in the bottom region of this compact (at 64 GPa) most of the compacted α-Si_3N_4 was transformed to strain free, fine β-Si_3N_4 grains after release of the shock pressure (Fig. 9b). As can be seen in Fig. 9b, these transformed β-Si_3N_4 grains are well consolidated together with remaining α-Si_3N_4 grains, though microhardness was reduced by this transformation.

Many studies have been carried out on the phase transformation of Si_3N_4 at high temperatures [18–21]. It has been reported that high-purity, CVD α-Si_3N_4, which is believed to contain no secondary phase in the structure, decomposed at high temperatures without a phase transformation to the β-form. Thus, the α-to-β phase transformation is only expected to occur through the intermedium of a liquid phase. Therefore, the transformation of α-Si_3N_4 to β-Si_3N_4 in the sample shock-loaded at 64 GPa suggests the presence of a liquid phase during the dynamic-compaction process. Furthermore, the maximum microhardness value obtained in this work, 21.2 GPa, which was a little lower than that of CVD α-Si_3N_4 as mentioned before, can imply that the degree of self-bonding in the compact was limited in some degree by the presence of a secondary phase at grain boundaries in the consolidation process. The liquid phase may be produced by the presence and reactions of impurities and a surface oxide layer (SiO_2) in the original powder. The transformed β-Si_3N_4 exhibited no residual strain, as mentioned before, indicating that the phase transformation took place at a residual temperature. Thus, it is considered that a liquid phase might have been produced during shock loading and remained after release of the shock pressure. The absence of conversion of α-Si_3N_4 to β-Si_3N_4 in the 44 GPa shocked sample seems to be due to the lower residual temperature at 44 GPa than at 64 GPa. It is, therefore, concluded that although no sintering aid was added intentionally to the original Si_3N_4 powder, small amounts of liquid phase resulting from impurities participated in the dynamic-compaction process at pressures above 44 GPa. The amount of the liquid

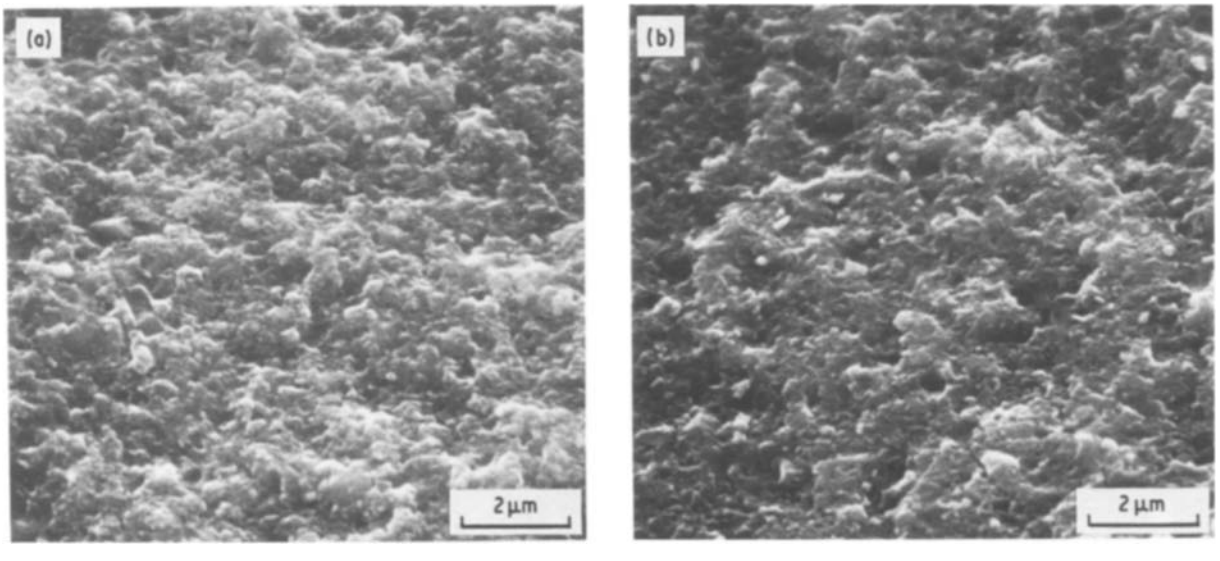

Figure 8 Scanning electron micrographs of a fracture surface of the 44 GPa shocked Si_3N_4: (a) front region; (b) bottom region.

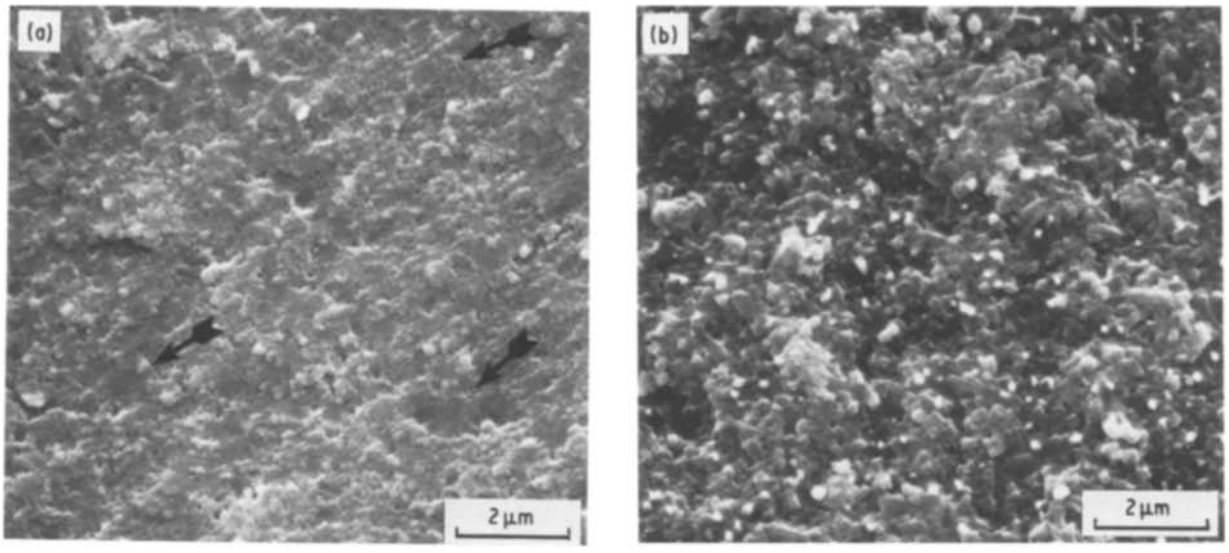

Figure 9 Scanning electron micrographs of a fracture surface of the 64 GPa shocked Si_3N_4: (a) front region; (b) bottom region.

phase which might have been produced during shock compression is estimated from the oxygen content in the starting material to be at least 2.4 wt%. The reaction between Si_3N_4 grains and the liquid at a high temperature seems to be important, but is unknown.

The presence of the secondary phase at grain boundaries degraded the strength of interparticle bonding of the Si_3N_4 compacts. However, the secondary phase, which might have been melted during shock compression, can provide a path for the fast diffusion of the species Si and N, resulting in an enhanced mass transport in the Si_3N_4 compact during the dynamic-compaction process. Furthermore, diffusion of the species can be enhanced by localized high temperature rises and the introduction of structural defects accompanied by plastic deformation at the time of densification. Rapid mass transport seems to enable the development of self-bonding between grains during an extremely short duration of the shock wave, $\simeq 1\ \mu$sec.

4. Conclusions

Si_3N_4 powder having no densification aids can be easily densified to 96% of the theoretical density by dynamic compaction at pressures of from 20 to 64 GPa, primarily by means of plastic deformation. In this pressure range microhardness values of the compacted Si_3N_4 powders are sensitive to the pressure and the α-to-β phase transformation.

The optimum shock pressure in the dynamic compaction of the Si_3N_4 powder with an initial density of 60% seems to be near 44 GPa, whereby a well-sintered Si_3N_4 compact with a density of 96% of the theoretical density and a microhardness of 21.2 GPa can be produced. The microhardness of the resulting Si_3N_4 compacts is reduced by the transformation to β-Si_3N_4.

The α-to-β phase transformation and microhardness values observed in the compacted Si_3N_4 suggest that small amounts of liquid phase participated in the dynamic compaction of the Si_3N_4 powder. Enhanced mass transport during shock compression due to the presence of the liquid phase at grain boundaries enables the rapid consolidation of Si_3N_4 grains during an extremely short duration of shock pressure. This results in the development of self-bonding in the powder compact.

References

1. C. GRESKOVICH and J. H. ROSOLOWSKI, *J. Amer. Ceram. Soc.* **59** (1976) 336.
2. G. E. GAZZA, *ibid.* **56** (1973) 662.
3. G. R. TERWILLIGER and F. F. LANGE, *ibid.* **57** (1974) 25.
4. A. TSUGE and K. NISHIDA, *Ceram. Bull.* **57** (1978) 424.
5. R. E. LOEHMAN and D. J. ROWCLIFFE, *J. Amer. Ceram. Soc.* **63** (1980) 144.
6. K. TSUKUMA, M. SHIMADA and M. KOIZUMI, *Ceram. Bull.* **60** (1981) 910.
7. K. NIIHARA, *ibid.* **63** (1984) 1160.
8. R. A. GRAHAM, B. MOROSIN, E. L. VENTURINI, E. K. BEAUCHAMP and W. F. HAMMETTER, in "Emergent Process Methods for High-Technology Ceramics" edited by R. F. Davis, H. Palmour III and R. L. Porter (Plenum Press, New York, 1984) p. 719.
9. J. J. PETROVIC, B. W. OLINGER and R. B. ROOF, *J. Mater. Sci.* **20** (1985) 391.
10. F. R. NORWOOD, R. A. GRAHAM and A. SAWAOKA, in "Shock Waves in Condensed Matter" edited by Y. M. Gupta (Plenum, New York, 1986) p. 837.
11. H. P. KLUG and L. E. ALEXANDER, "X-Ray Diffraction Procedures" (John Wiley, New York, 1975) p. 491.
12. C. P. GAZZARA and D. R. MESSIER, *Ceram. Bull.* **56** (1977) 777.
13. C. GRESKOVICH and G. E. GAZZA, *J. Mater. Sci. Lett.* **4** (1985) 195.
14. R. PRUMMER and G. ZIEGLER, *Powder Metall. Int.* **9** (1977) 11.
15. E. K. BEAUCHAMP, M. J. CARR and R. A. GRAHAM, *J. Amer. Ceram. Soc.* **68** (1985) 696.
16. T. AKASHI, V. LOTRICH, A. SAWAOKA and E. K. BEAUCHAMP, *ibid.* **68** (1985) C-322.
17. A. G. EVANS and R. W. DAVIDGE, *J. Mater. Sci.* **5** (1970) 314.
18. T. YAMADA, M. SHIMADA and M. KOIZUMI, *Ceram. Bull.* **60** (1981) 1281.
19. C. GRESKOVICH and S. PROCHAZKA, *J. Amer. Ceram. Soc.* **60** (1977) 471.
20. D. R. MESSIER, F. L. RILEY and R. J. BROOK, *J. Mater. Sci.* **13** (1978) 1199.
21. F. F. LANGE, *Ceram. Bull.* **62** (1983) 1369.
22. H. F. PRIEST, F. C. BURNS, G. L. PRIEST and E. C. SKAAR, *J. Amer. Ceram. Soc.* **56** (1973) 395.

Received 29 April
and accepted 21 July 1986